Experimental Evaluation of a Novel Sensor-Based Sorting Approach Featuring Predictive Real-Time Multiobject Tracking

Georg Maier , Florian Pfaff , *Member, IEEE*, Christoph Pieper, Robin Gruna ,
Benjamin Noack , *Member, IEEE*, Harald Kruggel-Emden, Thomas Längle ,
Uwe D. Hanebeck, *Fellow, IEEE*, Siegmar Wirtz, Viktor Scherer, and Jürgen Beyerer , *Member, IEEE*

Abstract—Sensor-based sorting is a machine vision application that has found industrial application in various fields. An accept-or-reject task is executed by separating a material stream into two fractions. Current systems use line-scanning sensors, which is convenient as the material is perceived during transportation. However, line-scanning sensors yield a single observation of each object and no information about their movement. Due to a delay between localization and separation, assumptions regarding the location and point in time for separation need to be made based on the prior localization. Hence, it is necessary to ensure that all objects are transported at uniform velocities. This is often a complex and costly solution. In this article, we propose a new method for reliably separating particles at nonuniform velocities. The problem is transferred from a mechanical to an algorithmic level. Our novel advanced image processing approach includes equipping the sorter with an area-scan camera in combination with a real-time multiobject tracking system, which enables predictions of the location of individual objects for separation. For the experimental validation of our approach, we present a modular sorting system, which allows comparing sorting results using a line-scan and area-scan camera. Results show that our approach performs reliable separation and hence increases sorting efficiency.

Index Terms—Automated visual inspection, machine vision, real-time multiobject tracking, sensor-based sorting.

G. Maier, R. Gruna, T. Längle, and J. Beyerer are with the Fraunhofer IOSB, 76131 Karlsruhe, Germany, and also with the Institute of Optronics, System Technologies and Image Exploitation, 76131 Karlsruhe, Germany (e-mail: georg.maier@iosb.fraunhofer.de; robin.gruna@iosb.fraunhofer.de; thomas.laengle@iosb.fraunhofer.de; juergen.beyerer@iosb.fraunhofer.de).

F. Pfaff, B. Noack, and U. D. Hanebeck are with the Intelligent Sensor-Actuator-Systems Laboratory, Karlsruhe Institute of Technology, 76131 Karlsruhe, Germany (e-mail: pfaff@kit.edu; noack@kit.edu; uwe.hanebeck@kit.edu).

C. Pieper, S. Wirtz, and V. Scherer are with the Department of Energy Plant Technology, Ruhr-Universität Bochum, 44801 Bochum, Germany (e-mail: pieper@leat.rub.de; wirtz@leat.rub.de; scherer@leat.rub.de).

H. Kruggel-Emden is with the Mechanical Process Engineering and Solids Processing, TU Berlin, 10623 Berlin, Germany (e-mail: kruggel-emden@tu-berlin.de).

Color versions of one or more of the figures in this article are available online at https://ieeexplore.ieee.org.

Digital Object Identifier 10.1109/TIE.2020.2970643

I. INTRODUCTION

SENSOR-BASED sorting is a machine vision application that is of high relevance in various industrial fields. Commonly, the task can be understood as performing an accept-or-reject decision with the goal to detect and remove defect, faulty, low quality, or foreign items from a stream of material in a production line [1]. Corresponding systems are typically used for quality inspection. The particular motivation depends on the field of application. For instance, in the field of mineral processing, the efficient extraction and recovery of raw materials is crucial due to limited existing reserves. Examples include the sorting of porphyry copper [2], quartz, magnesite, and gold ores [3], [4]. In food processing, products, e.g., dried vegetables, fruits [5], and nuts [6], often need to be cleaned from foreign, potentially dangerous objects as well as low quality and damaged entities. Furthermore, sensor-based sorting solutions are a key technology in recycling and are often implemented as part of waste processing with the goal to separate materials for reuse [7]. For instance, recent works propose usage for automated sorting of plastic flakes [8] and electronic waste [9]. In an industrial application, systems typically run 24 h a day, seven days a week, consequently handling massive amounts of the goods to be sorted. Hence, any improvements in sorting efficiency already have enormous economic and ecologic impact due to the large quantities involved.

A. Functional Principle

A schematic illustration of sensor-based sorting systems is provided in Fig. 1. Obviously, the design and implementation involve several disciplines and has hence attracted research from various perspectives. From an abstract point of view, the material is fed into the system onto a transportation mechanism, for instance, a convey or belt or chute. Although best practice strategies have been acquired, for instance, as presented in [10] regarding chutes, design choices typically depend on the product
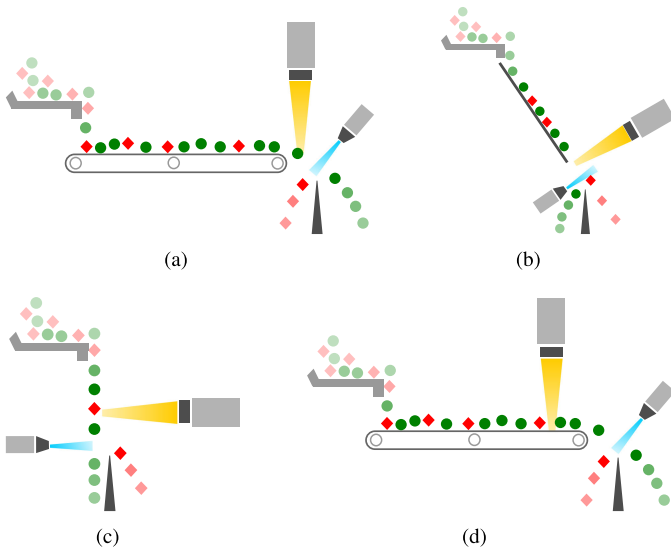
Fig. 1. Schematic illustration of common types of sensor-based sorting systems. The green objects represent particles to be accepted and the red ones those to be removed from the stream. The yellow ray denotes the field of view of the sensor and the blue ray the compressed air released to deflect an object. In Fig. 1(a) to (c), detection of particles happens during the flight phase. In contrast, in Fig. 1(d), detection happens on the transportation device. (a) Sorter with conveyor belt. (b) Sorter with chute. (c) Free fall sorter. (d) Sorter with conveyor belt.

to be sorted. Along the way, the material is perceived by one or multiple sensors, possibly in combination with an appropriate illumination device as for optical sensors [11]. State-of-the-art systems use line-scanning sensors for this purpose. Perception can take place either after the material has been discharged from the transport mechanism, as illustrated in Fig. 1(a) to (c), or while it is still on it, see Fig. 1(d). Sorting applications relying on high material throughput, as given in most industrial applications, typically use imaging sensors. Such types of systems require a real-time capable data processing pipeline, which typically consists of image acquisition, image preprocessing, feature extraction, classification, and actuator control. With respect to real-time requirements, firm deadlines apply for the deflection of objects since the actuators need to be triggered exactly when the objects pass the separation stage. Whenever this deadline is missed, these objects falsely remain in the accepted material. Besides monochrome and color cameras [3], [12], examples include X-ray transmission [13]–[16], near-infrared, and hyperspectral cameras [2], [17]–[19] as well as systems that combine different sensors [8], [16], [20]. An example for nonimaging sensors is the application of microphones, for instance, to characterize materials based on impact resonant acoustic emissions [8]. In this article, we are interested in the most common system type, i.e., systems using imaging sensors.

Data analysis is performed on the image with the goal to localize and classify the individual objects contained in the feed material. Based on the classification, a sorting decision is derived for each object. The choice of an appropriate sensor depends on the sorting task and the material's classification criteria at hand. Typically, the image data need to be preprocessed in a first step. Following that, the image is segmented and regions containing individual objects are extracted. Classification is performed on the basis of certain features, e.g., color or geometry related, and a sorting decision is derived. The decision is carried out by means of a separation mechanism. In theory, an arbitrary number of classes can be distinguished at the detection stage and separation into several fractions is possible. However, in industrial applications, the task is preferably realized as a binary sorting task, i.e., product and residues, since multiway sorting requires complex mechanical handling.

For the successful application of sensor-based sorting, the feed material is typically preconditioned in terms of using defined particle size distributions, which can be obtained via screening, for instance. Especially for small, cohesive materials, physical separation is typically performed using an array of compressed air nozzles [21], [22]. The minimum particle size that can be handled by a system is limited by the pneumatic resolution, proximity between objects and characteristics of the material transport. The system needs to be capable of deflecting single particles without causing any disturbances such as turbulence of other particles. For larger products, electromechanical fingers or robot arms are also used. However, in this article, we focus on pneumatic separation.

There are two main types of errors that can occur during the sorting process, potentially leading to a sorting error. The first type are errors in material recognition. In case of such an error, the data analysis reaches a wrong conclusion regarding the classification of a particle, which, for instance, can lead to the sorting decision of rejection although the particle was to be accepted. The second type are errors in material separation. Here, a correct sorting decision is derived, yet the particle is not physically removed from the product, for instance, due to poor control of the actuator. This is the type of error we focus on in this article, the recognition error is not considered.

B. Problem Formulation and Contribution

Besides the actual conveyance, the transportation phase aims at creating a monolayer of the material, i.e., avoid that particles lie on top of each other, decreasing proximity between individual objects, i.e., avoid the formation of clusters, and achieving ideal flow control. Creating a monolayer ensures that no occlusions occur. Avoiding proximity is important for the deflection of individual objects, since the pneumatic resolution, both spatial and temporal, is limited and codeflections of objects, i.e., the unwanted deflection of objects nearby an object that is to be deflected, are to be avoided. Ideal flow control means that all objects shall be accelerated to the same velocity, whereas velocity perpendicular to transport direction should be eliminated. This is crucial since there exists a temporal gap between the perception and the separation of the material, which is caused by the delay introduced by the required data processing, see Fig. 2. Localization is performed during perception and hence prior to separation. Due to usage of a line-scanning sensor, only a single image is available for each object. Therefore, no information regarding the motion of an object can be derived. Yet, in order to safely deflect objects that are to be removed from the stream, a prediction needs to be performed when and where they will reach
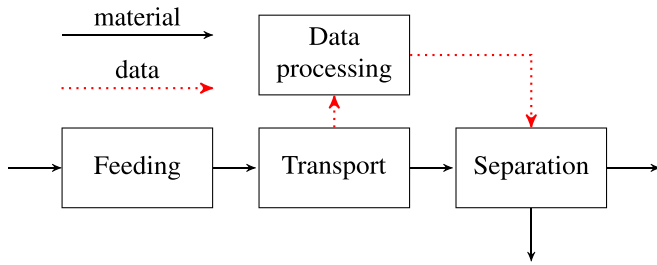
Fig. 2. Schematic workflow in sensor-based sorting. The schema illustrates that processing of the sensor data takes place while the material is still moving. Therefore, the location and point in time for separation need to be predicted during evaluation.
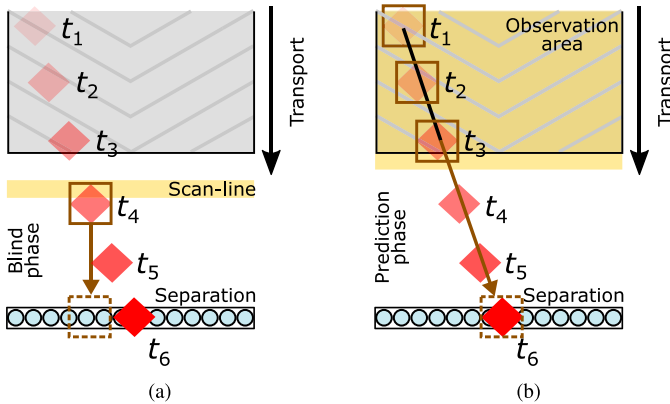

Fig. 3. Schematic illustration of the observation and separation process as seen from a view from above. The red rhombus represents a particle to be deflected at several time points. The box illustrates the localization as obtained from the image data and the dashed box the derived deflection pattern. (a) Line-scan system: The object is only observed at one time point and no motion information is available. This results in an error in separation. (b) Advanced image processing system: The object is observed several times. Motion information is used to calculate the deflection window.

the separation stage. Hence, a fixed delay between perception and separation is assumed for all particles. However, in the case of objects for which this assumption does not apply, an error may occur during separation, see Fig. 3(a).

One approach to minimize this error is to place the scan line as close as possible to the separation line. Although response times of sensors and processing systems are decreasing due to new developments, the distance cannot be arbitrarily minimized. Due to the firm real-time requirements, even in times of high system load caused by high material throughput, data processing needs to be completed before the material passes the separation stage. Even a few milliseconds of delay can cause the estimated position to differ from the actual position if there is no ideal flow control.

For certain materials, achieving optimal flow control is rather hard. A common strategy to increase the reliability of deflecting unwanted objects is to enlarge the deflection window, i.e., activate more nozzles longer than supposedly needed. However, this implies two major disadvantages. First, the risk of falsely codeflecting objects increases. Second, the amount of compressed air required to deflect the object increases. The latter is

particularly noteworthy considering the high energy demand and, hence, costs associated with the usage of compressed air [23]. In [24], it is estimated that about 70% of the operational costs of sensor-based sorting systems is caused by compressed air and air extraction. A mechanical solution to the problem is the application of very long convey or belts in order to gain more time during transportation for the material to come to rest. However, this solution is quite costly in terms of purchase costs, maintenance, and required space. Chutes are a much cheaper way of realizing transportation. In turn, achieving optimal flow control is comparatively hard. The texture and size of the contact surface of an individual object strongly impacts its motion along the chute.

In this article, we demonstrate how deviations in transport velocity can be handled by our advanced image processing approach instead of mechanical components. We present a sorting system equipped with an area-scan camera, a predictive real-time multiobject tracking system, and provide experimental results for the sorting efficiency in comparison with a conventional line-scan camera setup as contrasted in Fig. 3. Our system enables accurate, individual estimates per object where it is moving and even allows deriving information about how it is moving. Recent advances in CMOS camera technology support the suitability of our system for industrial application on a large scale. To our best knowledge, this is the first time a corresponding system was implemented and results of real sorting experiments are presented.

C. Related Work

The problem of tracking multiple objects has attracted intensive research over several decades, especially in the field of computer vision [25]. There exists a huge diversity of applications from different specialist areas in which input data for the tracking system is generated by an imaging sensor. Corresponding systems can be used to count entities in the field of view whereas entities appear and disappear over time, for instance, fish in underwater videos [26], vehicles for traffic flow surveillance [27], or people in video security applications [28]. Dependent on the system implementation, predictions of future events can be derived, for instance, collisions at traffic intersections [29]. In the context of quality control in an industrial setting, a system is proposed in [30] in which sputters are tracked during a laser-welding process. The system works at a comparatively high frame rate and has the purpose to detect only sputter events that are strong enough to be critical to the welding process. In the context of sensor-based sorting, utilizing multiobject tracking was first proposed in [31]. Using a simulation-driven approach [32], it was shown that predictive tracking can decrease the error in physical separation [33], [34].

Besides the mere detection and prediction of future events, tracking objects can also serve the purpose to perform quality assessment directly based on the motion behavior. Many works exist in the field of computer-assisted sperm analysis, both regarding animal [35] and human sperm quality [36]. The data from the tracking is here used to measure the motility of individual spermatozoa, which is an important characteristic for the

quality assessment [37]. In ecoinformatics, motion features can be used to classify certain species, for instance, birds [38]. In [39] and [40], tracking has also been proposed to utilize motion-based features for the characterization of materials in sensor-based sorting. This approach can enable the discrimination of optically identical products, although an optical sensor is used.

Many works exist discussing problems in characterization of materials in sensor-based sorting. However, evaluation of sorting systems from an holistic point of view appear to be rather rare. In [41], Pascoe *et al.* proposed a definition of separation efficiency and utilize it to quantify the sorting performance as a function of the proximity of objects in the material feed. They further investigate different feed characteristics by means of a Monte Carlo simulation and quantify results based on their prior introduced definition of sorting efficiency in [42]. Following the concept of receiver-operating characteristic curves, the idea of a sorting optimization curve (SOC) is presented in [43]. SOCs are intended to support the choice of an operating point based on yield and quality factors and predict the sorting quality. In [3], Gülcan and Gülsoy adapt the conventional approach of confusion matrices, which are typically used to evaluate a classifier to sensor-based sorting. This enables the usage of well-known figures of merit such as accuracy, specificity, and sensitivity.

II. METHODS AND MATERIALS

In this section, we provide a description of the methodological approach and the experimental platform that was designed for this study. In Section II-A, we outline the tracking system developed for sensor-based sorting. Following that, Section II-B introduces the sorting system designed for the evaluation.

A. Predictive Real-Time Multiobject Tracking

In contrast to conventional systems, which use line-scanning sensors, our system is based on the application of an area-scan sensor. The difference regarding the format of the obtained image data is illustrated in Fig. 4. When using line-scanning sensors, several lines recorded at consecutive time points are merged in order to obtain a 2-D image [44]. Hence, over time, an image of infinite length is formed. In turn, using an area-scan sensor yields a stack of 2-D images. The crucial difference is that using the area-scan sensor, individual objects can be detected at several time points, while line-scan sensor systems only obtain a single observation. In order to be able to track multiple objects simultaneously, the correspondences of objects in consecutive frames need to be determined. More precisely, for application in sensor-based sorting, several thousand objects need to be tracked concurrently. Hence, a multiobject tracking algorithm is used.

Individual objects in the feed are detected using image processing. More precisely, color-based segmentation in HSI color space is performed in order to convert a recorded color image in a segmentation image that partitions the image in multiple segments. Pixels belonging to the background are encoded with 0, while any other value represents a certain color class. In the course of this study, we define intervals for all three color components, i.e., hue, saturation, and intensity, to perform the
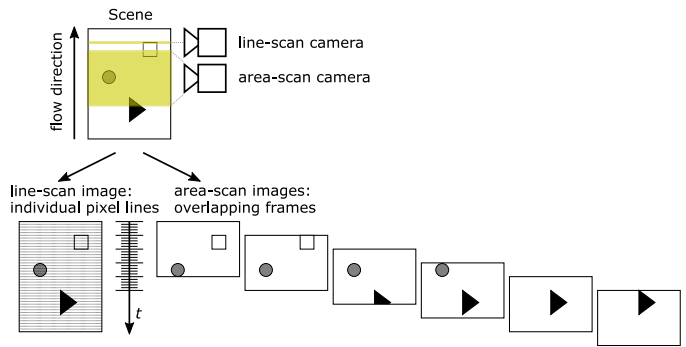

Fig. 4. Comparison of the image data as obtained via line-scan and area-scan sensors. Over time, the line-scan camera forms an image of infinite length composed of individual pixel lines, yielding only a single observation for each object. The are-scan camera acquires overlapping frames with partly redundant object information. Over time, objects are perceived at different positions at different time points. This allows deriving motion information.
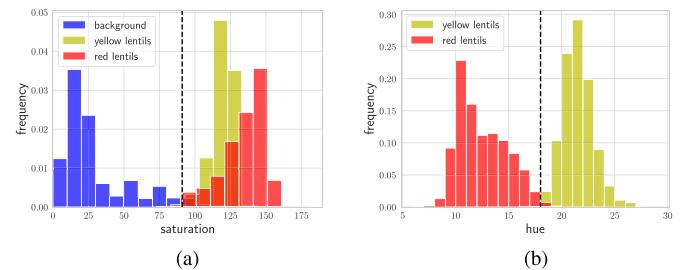

Fig. 5. Histograms show the ratio of occurrences of values for different objects in the image. They indicate that the image can be segmented based on color information, as depicted by the dashed lines. (a) Saturation of the background strongly differs from the one of the products. (b) Hue can be used to distinguish differently colored products, here: yellow and red lentils.

segmentation. As depicted in Fig. 5(a), segmentation into back- and foreground can be performed by defining a threshold for the saturation. A threshold for the hue enables distinguishing between different classes of objects, see Fig. 5(b). Including the intensity further improves the result.

Since there are typically several objects in an image, individual objects are identified using connected component analysis with an 8-connected neighborhood. Using this representation, we calculate the centroid. For an object covering n pixels with 2-D coordinates $p_i, i = 1, \ldots, n$, the centroid is calculated by $\frac{1}{n} \sum_{i=1}^{n} p_i$. The resulting point object serves as the input for the tracking algorithm. Hence, we perform point tracking, which is a common approach for tracking small objects in images [25].

In accordance to the categorization proposed in [45], our system implements a detection-based tracking approach with deterministic output. Moreover, results of the tracking are required in real time. Therefore, online tracking is performed, i.e., images are handled sequentially. We further refer to the system as *predictive* tracking since it enables predicting the point in time and position for the deflection of a particle. A schematic overview of the system is provided in Fig. 6.

For each object, a standard Kalman filter is used as an estimator, using the 2-D position $(x, y)^{\mathrm{T}}$ and the velocities in both
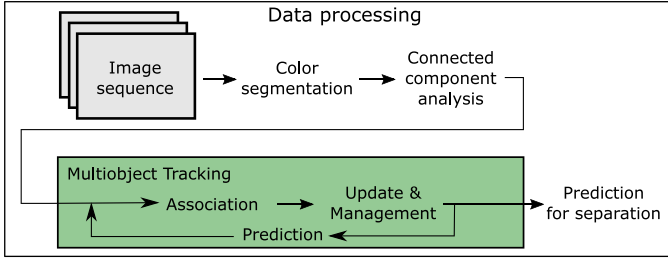
Fig. 6. Detailed view on the data processing block from Fig. 2. The system sequentially receives color images, which are first segmented based on color. Connected component analysis is then performed in order to identify individual objects in the image. The centroids of these objects serve as the input for the multiobject tracking system. The tracking system performs predictions for the currently existing tracks and identifies the correspondences between the predictions for and centroids of the current frame. It handles newly appeared and disappeared objects and provides the prediction for the separation.

directions, i.e., $(v_x, v_y)^T$, as state variables. When the assignments between measurements and tracks are known, knowledge about the positions of the objects is refined by performing a Kalman filter update step for each individual object. For the prediction step, we apply a linear motion model, more precisely a constant velocity model [46]. The underlying assumption of this model is that changes to the velocity are relatively small. For simplicity, the acceleration affecting the velocity is modeled as white noise, i.e., we assume the actual accelerations are temporarily independent and distributed according to the same probability distribution in every time step. It is important to note that the parameters of a motion model are estimated for each tracked object individually in each time step according to the movement observed so far. The complexity of the prediction step is $O(n)$ with n denoting the number of current tracks.

The point correspondences, i.e., the associations between predictions for and measurements of the current frame, are identified by solving the linear assignment problem

$$\min \quad \sum_{i=1}^{N} \sum_{j=1}^{M} a_{i,j} x_{i,j}$$

$$\text{s.t.} \quad \sum_{j=1}^{M} x_{i,j} = 1, \, i = 1, \dots, N$$

$$\sum_{i=1}^{N} x_{i,j} = 1, \, j = 1, \dots, M, \quad (1)$$

where N and M represent the number of predictions and measurements, respectively. The cost function a is implemented as the Mahalanobis distance. The constraints guarantee a one-to-one assignment. This problem needs to be solved for each frame and causes the main computational burden within the tracking algorithm. Due to its suitability for parallelization, we use the Auction Algorithm [47] for this purpose. An example image sequence highlighting results of the detection and tracking stages is provided in Fig. 7.

In each time step, we estimate the remaining time until an object will reach the separation stage. Whenever this estimated
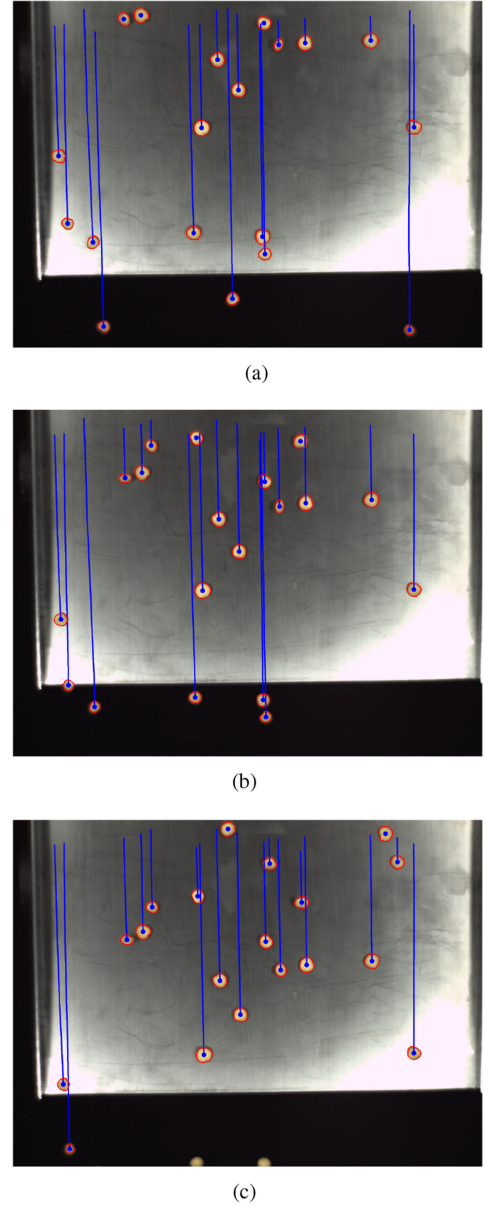

Fig. 7. Three consecutive frames as recorded by the system. The flow direction of the material is from top to bottom. The detected objects are highlighted by a red border. The blue circles indicate the current centroids of the objects and the blue lines the trajectories that the particles have followed so far. (a) Frame at t_n. (b) Frame at t_{n+1}. (c) Frame at t_{n+2}.

time gap reaches a certain threshold, the estimated point in time as well as position when the object reaches the separation stage is calculated and transmitted to the separation device. This threshold is required since it is necessary to transfer the deflection pattern with some advance to compensate for the delay induced by the transfer itself as well as the reaction time of the air valves.

With respect to real-time requirements on the system, it is important to note that the tracking and performing of predictions for separation are not only required to work synchronously with the image acquisition, but firm real-time requirements apply. A sorting decision can only be carried out until an object to

be deflected passed the separation mechanism. This results in a binary utility function, where the utility drops to zero after the deadline is missed. Therefore, we implement our system in C++ and exploit parallel processing on the CPU as well as a graphics processing unit (GPU). For instance, the Kalman filter update steps can be performed concurrently for all objects that are currently being tracked. Also, we use the optimized Auction Algorithm proposed in [48] for solving the linear assignment problem that is designed for running on a GPU and is particularly fast due to the usage of optimized data structures. The results presented in [48] show that the algorithm is capable of solving the association problem for about 1000 objects at around 200 Hz on a modern GPU. The algorithm is further robust against missed and faulty detections, which may be caused by occlusions, collisions are poor objects detection. This is achieved by implementing a scoring system for the creation of new tracks as well as the deletion of existing tracks. Each newly created track is assigned an initial score, which is increased whenever a measurement is assigned to the track until a defined maximum score is reached. In turn, if no measurement of a frame is assigned to the track, the score is decreased. In case the score drops below zero, the track is deleted. New tracks are created for measurements that have not been assigned to a track.

B. Experimental Optical Sorting Platform

For the validation of our approach, alterations on the hardware of the sorting system are required. More precisely, the system needs to be equipable both with a line-scan and an area-scan camera as well as the corresponding illumination devices. Therefore, for our experiments, we developed a system that enables rapid prototyping in this respect. A photo of the resulting construction is provided in Fig. 8.

1) General design: The basis of the sorting system is the back panel. It is realized as a mechanical breadboard and contains equidistant perforations that are intended for mounting different components. The distance between two perforations is 25 mm, both horizontally and vertically. The size of the board used in this study is 142 cm × 102 cm. Adapters are designed to build an interface between the back panel and commercially available components.

An electromagnetic feeder, annotated by 1 in Fig. 8, is used to feed material into the system. It runs at a constant frequency of 50 Hz. The amplitude is configurable via a controller containing a potentiometer and is monitored using a vibration sensor. The latter ensures a constant feeding rate, for instance, independent of the temperature of the electromagnetic feeder. The chute considered in this article has a total length of 31 cm and width of 15 cm, see annotation 2 in Fig. 8. It is made of cold-rolled steel and hence has a plain and even surface. The illumination for use with a line-scan camera (see 3(a) in Fig. 8) consists of two line-shaped LED bars, which are indicated by 3(b) in Fig. 8. It is mounted at a position such that the material is observed after falling off the chute. For usage with the area-scan camera, an LED ring light with an inner diameter of 21 cm is used. The observation area and consequently the position of the ring light are located at the end of the chute, see Fig. 7. In both cases, the
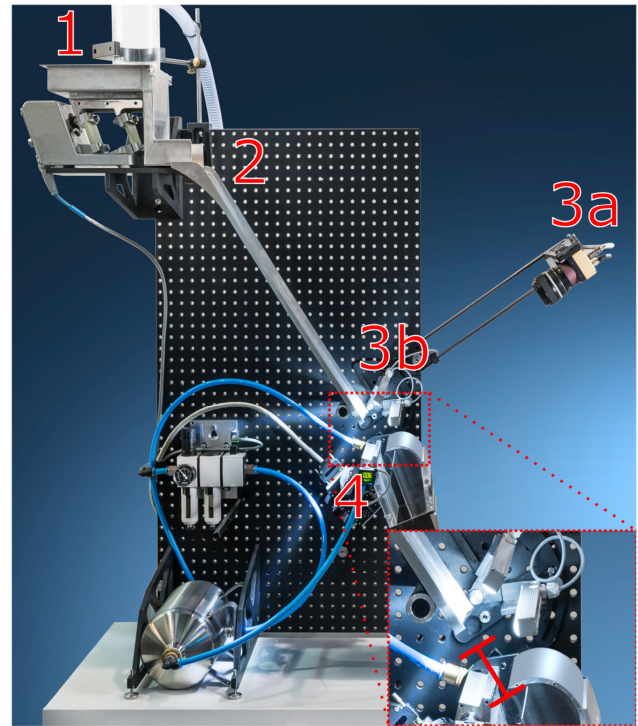

Fig. 8. Photo of our experimental system in the laboratory. The setup corresponds to the scheme provided in Fig. 1(b). The components as chronologically passed by the feed material are highlighted as follows: 1: vibrating feeder, 2: chute, 3a: sensor (here: line-scan camera), 3b: illumination (here: LED bars), 4: array of compressed air nozzles. The red line segment further illustrates the gap between perception and separation of the material.

bright field illumination is mounted above the material stream such that the reflected light is captured by the camera. Separation of the material is performed by fast switching compressed air valves. The system contains an array of 16 valves covering a distance of 16 cm, which can be activated individually, see 4 in Fig. 8. Hence, the spatial pneumatic resolution is 10 mm. The pressure can be controlled using a pressure regulator. The individual valves are accessed via a controller area network (CAN). The speed of communication over the data channel, i.e., the baud rate, is 1000 bd.

2) Image acquisition: For the comparison of sorting efficiency, experiments are carried out with a line-scan and an area-scan camera. In both cases, the reflected light from the particles is captured by the camera sensor. This can be used to measure color features. The line-scan model used is *e2v AViiVa SC2*, which offers 1365 px at a maximum line rate of 14.8 kHz. The area-scan model used is *Allied Vision Bonito CL-400 color* camera, which offers a maximum resolution of 2320 × 1726 px at 192 Hz. For both cameras, we use the *Zeiss Classic lense Planar T 1.4/50 ZF.2*. Both cameras are connected to a computer using the *Camera Link* interface. Therefore, the computer is also equipped with a programmable frame grabber from the *microEnable 4 series* from *Silicon Software*. Several image preprocessing steps are performed directly on the grabber, such as shading, demosaicing (for the area-scan camera), and generation of the segmentation image.

Fig. 9. Products used for the experiments conducted. (a) Wooden plates. (b) Lentils.

3) Processing computer system:

The computer system is equipped with an *Intel i7-5960X CPU* and 16 GB RAM. Furthermore, it contains a *NVIDIA GeForce GT 740* GPU on which the association step for multiobject tracking is performed. The operating system is *Microsoft Windows 7 64-bit*.

III. TEST METHODOLOGY

In order to allow a fair comparison between the conventional and our proposed approach, we ensure that all operational sorting parameters are fixed except for the changes to components owed to the approaches themselves, e.g., illumination, sensor, and data processing. This implies that we are not interested in presenting an optimal sorting solution for a specific product, but rather in demonstrating that the proposed approach can increase sorting performance in a relative fashion. In the following sections, the relevant sorting parameters considered in the study are described.

A. Characteristics of the Material Stream

We perform sorting experiments for two artificially labeled products: wooden plates and dry lentils, see Fig. 9. The products were deliberately chosen due to major differences in geometry and movement behavior on the chute. More precisely, the wooden plates represent a very homogeneous and the lentils a highly heterogeneous product in terms of the shape of individual particles. A thorough description of the wooden plates can be found in [32]. Their volume is 2 mm × 5 mm × 6 mm. The plates are artificially separated into two fractions by coloring, whereas some plates are kept wooden and some are colored blue. Being a natural product, the volume of the lentils is diverse. However, most lentils have a diameter of approximately 4 mm. In order to derive a sorting decision, we include yellow and red lentils in the material stream. Hence, for both products, a significant difference in color exists to discriminate the product into two fractions. For our experiments, this allows us to neglect recognition errors because they do not occur and solely measure the error in physical separation.

An experiment carried out consists of sorting 200 g of the product in a batchwise manner. The mass flow of the material in our scenario depends on the amplitude of the feeder. We investigate a single configuration of the feeder that results in a similar mass flow for both products. The mass flow was determined experimentally by feeding material through the system onto a digital weighing scale, which is connected to a computer in order to record the measured values over time at a temporal resolution

of approximately 18 Hz. After starting the feeding process, the mass flow increases over time until reaching approximately 5 gs^{-1}. Most of the time of the sorting process, the feeding rate remains in this state. When only little material is left in the feeder, the mass flow decreases until no material is left. With respect to the amount of material to be deflected, we consider a ratio of 5%. The impact of the mass flow and ratio to be deflected on sorting performance has already occasionally been investigated in the literature, e.g., [41], [42].

B. Sensor and Software Parameters

We configure the line-scan camera to run at approximately 7682 Hz using a width of 446 pixels. Due to the high required data transfer rate and the resulting computational burden, we restrict the area-scan camera to approximately 93 fps. Consequently, the entire data processing, i.e., demosaicing the Bayer pattern, color segmentation, connected component analysis, descriptor extraction, tracking, classification and transfer of deflection patterns, is granted a processing time of approximately 10 ms on average. Furthermore, the image is cropped to a width of 2208 pixels. For the area-scan camera, we report a spatial resolution of approximately 69.58 μm and for the line-scan camera of 359.65 μm. It is important to note that the difference is negligible as for both cases the spatial resolution is many times higher than the pneumatic spatial resolution.

The deflection pattern describes which nozzles are to be triggered during which time interval. There exist different approaches how the pattern can be calculated [49]. As also done in [42], we use the common approach of using the bounding box of an object to be deflected to calculate the deflection pattern. However, we consider two configurations. The first configuration corresponds to the bounding box of the object as detected in the image and is referred to as *small pattern* in the remainder. The second configuration uses enlarged deflection patterns and is referred to as *large pattern* in the remainder. Here, the window is enlarged both in transport direction and perpendicular to it. In perpendicular direction, we enlarge the window on both sides by 5 mm, which is motivated by the fact that this corresponds to half the area covered by a single valve and hence implies activation of the neighboring valve on both sides. With respect to enlargement in transport direction, we configure an individual parameter per product. This is motivated by the empirical observation that the deviations in velocity in transport direction v_y, i.e., down the chute, are noticeably larger for wooden plates than for lentils. For wooden plates, we extend the window timewise by 7.5 ms and for lentils by 2.2 ms before the start and after the end of the object as described by the estimated bounding box. As has been mentioned in Section I-B, enlarging the deflection pattern can be used to achieve more reliable deflections. However, it comes at the cost of increasing the risk of falsely codeflecting objects located nearby and increases the amount of compressed air required.

C. Mechanical Parameters

The distance between the observation line of the line-scan camera and the separation is approximately 34 mm. When using

the area-scan camera, the pixel row located closest to the separation lies approximately 18 mm in front of it. As mentioned in Section II-A, the predicted deflection pattern of an object to be rejected is transmitted to the separation device whenever the estimated time remaining until reaching the separation stage falls below a certain threshold. In our system, this time threshold is formulated as a multiple k of the duration of a single frame t_{frame}. The time threshold is then given by

$$\theta := kt_{\text{frame}}. \qquad (2)$$

Obviously, it is desirable to set the time threshold as small as possible in order to use the most recent information of an object for the calculation of the pattern. However, an existing delay in transmitting the information and physically activating a valve needs to be considered. The average distance $\overline{d}$ of the last observation point to the separation is calculated by

$$\overline{d} = \theta \overline{v_y} \qquad (3)$$

where $\overline{v_y}$ denotes the average velocity in transport direction. In the following scenarios, k is set to 2.5, which approximately yields 26.9 ms for θ and was determined empirically. Both for wooden plates and lentils, this yields $\overline{d} \approx 47$ mm and, hence, a greater distance than the line-scan camera setup, which leads to a potential disadvantage. The distance between perception and separation together with the average velocity in transport direction can also be used to configure the delay for the line-scan camera system. For both products, dividing the distance by the mean velocity yields a delay of approximately 19 ms. However, an additional activation delay of the valves needs to be considered. Although vendors supply corresponding delay times, those are typically determined under very stable and ideal conditions, for instance, regarding temperature, pressure, and power supply [50]. Therefore, the trigger delay was determined empirically for the system at hand and was found to be around 3 ms. Hence, the delay configured is 16 ms.

Besides these separation related parameters, the angle of the chute has a large impact on transportation characteristics. For the experiments presented in this article, the chute was mounted with an angle of $54°$. This angle was found empirically to yield a good transportation of the products.

D. Definition of Sorting Efficiency

We adapt the definition of sorting efficiency from [41], [42] which is formulated as

$$\text{Separation efficiency (SE) } \% := R_d - R_c \qquad (4)$$

where R_d is the ratio of objects to be rejected and, hence, to be deflected that are located in the reject bin (true positive) in percent and R_c is the ratio of objects to be accepted that are also located in the reject bin (false positive) after the sorting process and, hence, were codeflected in percent. In our definition, *positive* describes the test result for residues. The development of the key figure SE has recently been discussed in [51]. Obviously, in order to determine R_d and R_c, the fraction of objects belonging to the accept and reject class needs to be determined per bin. In the course of this article, we reapply the two separate bins after the sorting process on the sorting system and use the image

processing algorithms to count the number of objects per class in the stream. The material is not separated again.

The outcome of the sorting process is not deterministic and is exposed to stochastic fluctuations. Various factors can impact the sorting efficiency even when keeping the parameters static. For instance, the material mixing is not identical when performing several runs, the mass flow can slightly vary, etc. Such differences can also influence the proximity between objects, which is known to have an impact on the sorting efficiency [41]. Therefore, every experiment was repeated 20 times and statistics were calculated.

IV. EXPERIMENTAL RESULTS

Sorting results for wooden plates and lentils are illustrated in Figs. 10 and 11, respectively, and provided quantitatively in Table I. Regarding the discussion of results, it is emphasized that we are less interested in the absolute sorting efficiency but rather in a relative view, comparing the two system types.

Results for wooden plates using the small deflection pattern clearly reveal the disadvantage of using a static assumption regarding the separation delay when dealing with scenarios with high deviations in velocity. This disadvantage is clearly reflected in the performance of the line-scan camera system, see Fig. 10(a). The tracking system achieves considerably higher sorting performance in this case, quantitatively by over 11 percentage points in average. This is due to a better outcome in R_d. Results with respect to R_c are almost equal, see Table I. Enlarging the deflection pattern increases R_d for both system types, whereas the improvement is greater for the line-scan camera system, see Fig. 10(b). In average, R_d is increased by almost 12 percentage points for the line-scan camera based system and almost 3 percentage points for the tracking approach. The tracking system still achieves a higher sorting efficiency, however, the difference drops to just over 2 percentage points in average. Hence, the performances of the systems are getting closer to one another. However, this comes at the cost of higher energy consumption due to the increased usage of compressed air. For both system types, there exist experiments for which $R_d > 90\%$ can be reported. Yet it also holds true that R_c is increased in this case.

Experiments carried out with lentils yield similar results. Yet, the difference in sorting efficiency is even bigger when using small deflection patterns, see Fig. 11(a), namely approximately 20 percentage points in average. The difference is again mainly due to superior results of the tracking system in R_d. Employing large deflection patterns leads to convergence of the system's performances as has been the case with wooden plates, see Fig. 11(b). Yet, the difference in mean sorting efficiency still lies around 7 percentage points in this case. In general, it appears that lentils are a harder sorting task than wooden plates. We do not elaborate further on this assumption but refer to the work presented in [49], which suggests that the mere smaller size of the objects may increase difficulty, as well as to the higher diversity in shape.

The distributions of the markers in Figs. 10 and 11 underline the previous statement that sorting results may vary from batch to batch. However, by repeating each experiment 20 times and
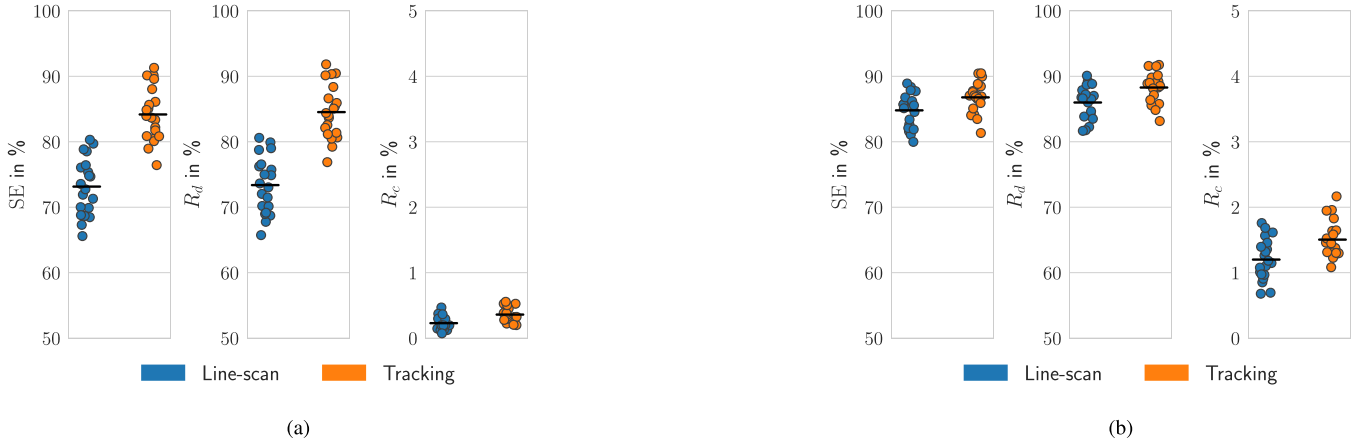
Fig. 10. Sorting results for wooden plates. The markers denote the results of the individual experiments and the black horizontal bar the mean. (a) Small deflection pattern. (b) Large deflection pattern.
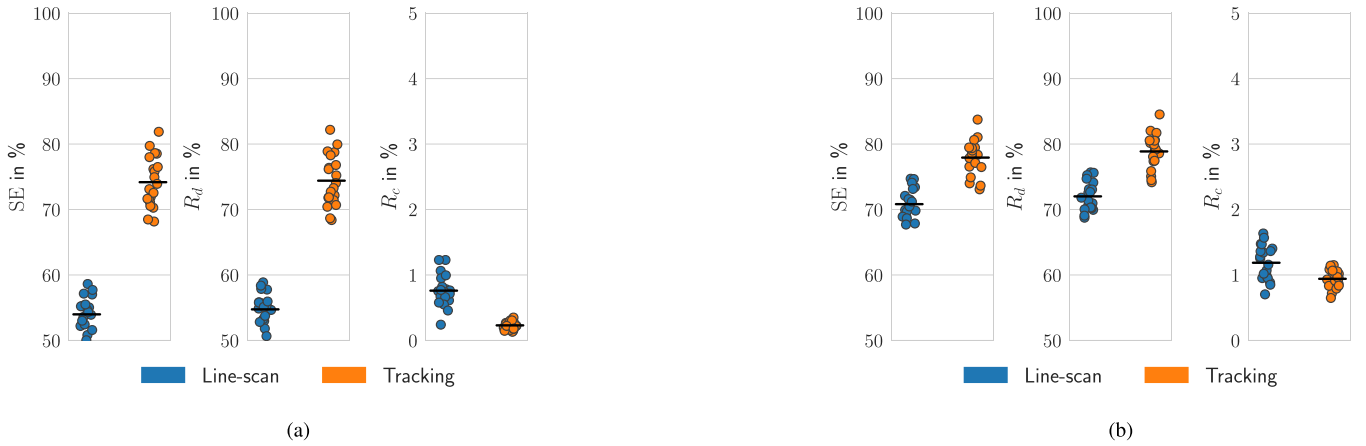

Fig. 11. Sorting results for lentils. The markers denote the results of the individual experiments and the black horizontal bar the mean. (a) Small deflection pattern. (b) Large deflection pattern.

TABLE I
DETAILED RESULTS FOR THE SORTING EXPERIMENTS CONDUCTED

Product	Deflection pattern	System	$\overline{R_d}$	$\overline{R_c}$	$\overline{SE}$	$\Delta\overline{SE}$
Plates	small	Line-scan	73.38	0.23	73.15	11.02
		Tracking	84.53	0.36	84.17	
	large	Line-scan	86.00	1.20	84.80	1.98
		Tracking	88.29	1.51	86.78	
Lentils	small	Line-scan	54.74	0.76	53.98	20.19
		Tracking	74.40	0.23	74.17	
	large	Line-scan	72.01	1.19	70.82	7.11
		Tracking	78.87	0.94	77.93	

taking the average, our results are stable enough to conclude that the sorting approach including an area-scan camera and tracking outperforms the conventional setup including a line-scan camera in each scenario. The increase in sorting efficiency is particularly high when working with small deflection patterns. This is of no surprise since large deflection patterns are a well-established measure taken to compensate imperfect flow control. In addition to the increased use of compressed air, it can also be

observed from the results that enlarging the deflection pattern has a negative impact on R_c as has been claimed before.

V. CONCLUSION

In this article, we proposed an advanced image processing approach for decreasing the error in physical separation in sensor-based sorting. Our method enables reliable deflection of objects even at nonuniform velocities of individual objects. For this purpose, we proposed equipping a sorting system with an area-scan sensor and a predictive real-time multiobject tracking system. Based on experimentation with two different sorting tasks, we have shown that the proposed system outperforms a state-of-the-art reference system in every configuration under consideration. Sorting efficiency was increased by at least 2 percentage points and at most 20 percentage points. The increased efficiency is a result of the higher deflection accuracy. It was further shown that the proposed approach allows for employing small deflection patterns while retaining the sorting efficiency, which in turn lowers the required amount of compressed air and, hence, improves profitability and environmental friendliness.

This article revealed the necessity for accelerating computations of our advanced image processing system in order to achieve higher throughput for practical applications. Especially in case of the desired transfer from our experimental sorting system to an industrial sized system, real-time related issues might become more challenging since more objects need to be tracked, classified, and separated simultaneously. Furthermore, our system not only provides information regarding where an object is moving but also how it is moving. We consider utilizing motion information for the identification of the materials in real sorting scenarios as proposed in [39] and [40] to be a promising research direction.

REFERENCES

[1] E. N. Malamas, E. G. Petrakis, M. Zervakis, L. Petit, and J.-D. Legat, "A survey on industrial vision systems, applications and tools," *Image Vis. Comput.*, vol. 21, no. 2, pp. 171–188, 2003.

[2] M. Dalm, M. W. Buxton, F. J. van Ruitenbeek, and J. H. Voncken, "Application of near-infrared spectroscopy to sensor based sorting of a porphyry copper ore," *Minerals Eng.*, vol. 58, pp. 7–16, 2014.

[3] E. Gülcan and Ö. Y. Gülsoy, "Performance evaluation of optical sorting in mineral processing–A case study with quartz, magnesite, hematite, lignite, copper and gold ores," *Int. J. Mineral Process.*, vol. 169, pp. 129–141, 2017.

[4] T. Phiri, H. J. Glass, and P. Mwamba, "Development of a strategy and interpretation of the NIR spectra for application in automated sorting," *Minerals Eng.*, vol. 127, pp. 224–231, 2018.

[5] S. Cubero, N. Aleixos, E. Moltó, J. Gómez-Sanchis, and J. Blasco, "Advances in machine vision applications for automatic inspection and quality evaluation of fruits and vegetables," *Food Bioprocess Technol.*, vol. 4, no. 4, pp. 487–504, 2011.

[6] T. Pearson and N. Toyofuku, "Automated sorting of pistachio nuts with closed shells," *Appl. Eng. Agriculture*, vol. 16, no. 1, 2000, Art. no. 91.

[7] S. P. Gundupalli, S. Hait, and A. Thakur, "A review on automated sorting of source-separated municipal solid waste for recycling," *Waste Manage.*, vol. 60, pp. 56–74, 2017.

[8] J. Huang, C. Tian, J. Ren, and Z. Bian, "Study on impact acoustic–visual sensor-based sorting of ELV plastic materials," *Sensors*, vol. 17, no. 6, 2017, Art. no. 1325.

[9] S. P. Gundupalli, S. Hait, and A. Thakur, "Classification of metallic and non-metallic fractions of e-waste using thermal imaging-based technique," *Process Saf. Environmental Protection*, vol. 118, pp. 32–39, 2018.

[10] D. Stuart-Dick and T. Royal, "Design principles for chutes to handle bulk solids," *Bulk Solids Handling*, vol. 12, pp. 447–447, 1992.

[11] R. Gruna and J. Beyerer, "Feature-specific illumination patterns for automated visual inspection," in *Proc. IEEE Int. Instrum. Meas. Technol. Conf.*, Graz, Austria, May 2012, pp. 360–365.

[12] T. Pearson, "High-speed sorting of grains by color and surface texture," *Appl. Eng. Agriculture*, vol. 26, no. 3, pp. 499–505, 2010.

[13] J. Lessard, J. de Bakker, and L. McHugh, "Development of ore sorting and its impact on mineral processing economics," *Minerals Eng.*, vol. 65, pp. 88–97, 2014.

[14] M. Meirhofer, G. Piringer, D. Rixrath, M. Sommer, and A. M. Ragossnig, "Implementing an advanced waste separation step in an MBT plant: assessment of technical, economic and environmental impacts," *Waste Manage. Res.*, vol. 31, no. 10_suppl, pp. 35–45, 2013.

[15] L. Von Ketelhodt and C. Bergmann, "Dual energy X-ray transmission sorting of coal," *J. Southern African Inst. Mining Metall.*, vol. 110, no. 7, pp. 371–378, 2010.

[16] M. Mesina, T. De Jong, and W. Dalmijn, "Automatic sorting of scrap metals with a combined electromagnetic and dual energy X-ray transmission sensor," *Int. J. Mineral Process.*, vol. 82, no. 4, pp. 222–232, 2007.

[17] M. Dalm, M. Buxton, and F. Van Ruitenbeek, "Applicability of near-infrared hyperspectral imagery (NIR-HI) for sensor based sorting of an epithermal Au-Ag ore," in *Proc. 54th Annu. Conf. Metallurgists*, Toronto, ON, Canada, Aug., 2015, pp. 1–12.

[18] M. Dalm, M. Buxton, and F. van Ruitenbeek, "Discriminating ore and waste in a porphyry copper deposit using short-wavelength infrared (SWIR) hyperspectral imagery," *Minerals Eng.*, vol. 105, pp. 10–18, 2017.

[19] F. Hollstein, Í. Cacho, S. Arnaiz, and M. Wohllebe, "Challenges in automatic sorting of construction and demolition waste by hyperspectral imaging," *Proc. SPIE*, vol. 9862, 2016, Art. no. 98620J.

[20] H. Kattentidt, T. De Jong, and W. Dalmijn, "Multi-sensor identification and sorting of bulk solids," *Control Eng. Pract.*, vol. 11, no. 1, pp. 41–47, 2003.

[21] T. Ferreira, S. Sesmat, E. Bideaux, and F. Sixdenier, "Experimental analysis of air jets for sorting applications," in *Proc. 8th FPNI Ph.D Symp. Fluid Power*, pp. V001T01A007–V001T01A007, 2014.

[22] T. Ferreira, S. Sesmat, E. Bideaux, and F. Sixdenier, "Fast switching pneumatic valves: Experimental bench for flow and pulsed air jet characterizations," in *Proc. 13th Scand. Int. Conf. Fluid Power*, 2013, pp. 457–464.

[23] R. Saidur, N. Rahim, and M. Hasanuzzaman, "A review on compressed-air energy use and energy savings," *Renewable Sustain. Energy Rev.*, vol. 14, no. 4, pp. 1135–1153, May 2010.

[24] E. Gülcan and Ö. Y. Gülsoy, "Optical sorting of lignite and its effects on process economics," *Int. J. Coal Preparation Utilization*, vol. 38, no. 3, pp. 107–126, 2018.

[25] A. Yilmaz, O. Javed, and M. Shah, "Object tracking: A survey," *ACM Comput. Surv.*, vol. 38, no. 4, 2006, Art. no. 13.

[26] C. Spampinato, Y.-H. Chen-Burger, G. Nadarajan, and R. B. Fisher, "Detecting, tracking and counting fish in low quality unconstrained underwater videos," *VISAPP*, vol. 2008, pp. 514–519, 2008.

[27] L. Unzueta, M. Nieto, A. Cortés, J. Barandiaran, O. Otaegui, and P. Sánchez, "Adaptive multicue background subtraction for robust vehicle counting and classification," *IEEE Trans. Intell. Transp. Syst.*, vol. 13, no. 2, pp. 527–540, Jun. 2012.

[28] L. Snidaro, C. Micheloni, and C. Chiavedale, "Video security for ambient intelligence," *IEEE Trans. Syst., Man, Cybern.—Part A, Syst. Humans*, vol. 35, no. 1, pp. 133–144, Jan. 2005.

[29] S. Atev, H. Arumugam, O. Masoud, R. Janardan, and N. P. Papanikolopoulos, "A vision-based approach to collision prediction at traffic intersections," *IEEE Trans. Intell. Transp. Syst.*, vol. 6, no. 4, pp. 416–423, Dec. 2005.

[30] M. Jager, S. Humbert, and F. A. Hamprecht, "Sputter tracking for the automatic monitoring of industrial laser-welding processes," *IEEE Trans. Ind. Electron.*, vol. 55, no. 5, pp. 2177–2184, May 2008, http://dx.doi.org/10.1109/TIE.2008.918637 DOI 10.1109/TIE.2008.918637.

[31] F. Pfaff *et al.*, "TrackSort: Predictive tracking for sorting uncooperative bulk materials," in *Proc. IEEE Int. Conf. Multisensor Fusion Integration Intell. Syst.*, 2015, pp. 7–12.

[32] C. Pieper *et al.*, "Numerical modeling of an automated optical belt sorter using the discrete element method," *Powder Technol.*, vol. 301, pp. 805–814, 2016.

[33] F. Pfaff *et al.*, "Simulation-based evaluation of predictive tracking for sorting bulk materials," in *Proc. IEEE Int. Conf. Multisensor Fusion Integration Intell. Syst.*, 2016, pp. 511–516.

[34] C. Pieper *et al.*, "Numerical modelling of an optical belt sorter using a DEMCFD approach coupled with particle tracking and comparison with experiments," *Powder Technol.*, vol. 340, pp. 181–193, 2018.

[35] D. Kime, K. Van Look, B. McAllister, G. Huyskens, E. Rurangwa, and F. Ollevier, "Computer-assisted sperm analysis (CASA) as a tool for monitoring sperm quality in fish," *Comparative Biochem. Physiol. Part C, Toxicol. Pharmacol.*, vol. 130, no. 4, pp. 425–433, 2001.

[36] L. Sørensen, J. Østergaard, P. Johansen, and M. de Bruijne, "Multi-object tracking of human spermatozoa," *Proc. SPIE*, vol. 6914, pp. 6914–6914, 2008.

[37] J. Liu, C. Leung, Z. Lu, and Y. Sun, "Quantitative analysis of locomotive behavior of human sperm head and tail," *IEEE Trans. Biomed. Eng.*, vol. 60, no. 2, pp. 390–396, Feb. 2013.

[38] J. Atanbori, W. Duan, E. Shaw, K. Appiah, and P. Dickinson, "Classification of bird species from video using appearance and motion features," *Ecological Inform.*, vol. 48, pp. 12–23, 2018.

[39] G. Maier *et al.*, "Improving material characterization in sensor-based sorting by utilizing motion information," in *Proc. Opt. Characterization Mater. Conf. Proc.*, 2017, p. 109.

[40] G. Maier *et al.*, "Motion-based material characterization in sensor-based sorting," *tm-Technisches Messen*, vol. 85, no. 3, pp. 202–210, 2018.

[41] R. Pascoe, O. B. Udoudo, and H. Glass, "Efficiency of automated sorter performance based on particle proximity information," *Minerals Eng.*, vol. 23, no. 10, pp. 806–812, 2010.

[42] R. Pascoe, R. Fitzpatrick, and J. Garratt, "Prediction of automated sorter performance utilising a Monte Carlo simulation of feed characteristics," *Minerals Eng.*, vol. 72, pp. 101–107, 2015.

[43] D. Ooms, R. Palm, V. Leemans, and M.-F. Destain, "A sorting optimization curve with quality and yield requirements," *Pattern Recognit. Lett.*, vol. 31, no. 9, pp. 983–990, 2010.

[44] E. Gülcan and Ö. Y. Gülsoy, "Evaluation of complex copper ore sorting: Effect of optical filtering on particle recognition," *Minerals Eng.*, vol. 127, pp. 208–223, 2018.

[45] W. Luo, X. Zhao, and T. Kim, "Multiple object tracking: A literature review," 2017, *arXiv:1409.7618*. [Online]. Available: http://arxiv.org/abs/1409.7618v4

[46] X. R. Li and V. P. Jilkov, "Survey of maneuvering target tracking. Part I. Dynamic models," *IEEE Trans. Aerosp. Electron. Syst.*, vol. 39, no. 4, pp. 1333–1364, Oct. 2003.

[47] D. P. Bertsekas, "The auction algorithm: A distributed relaxation method for the assignment problem," *Ann. Oper. Res.*, vol. 14, no. 1, pp. 105–123, 1988.

[48] G. Maier *et al.*, "Real-time multitarget tracking for sensor-based sorting," *J. Real-Time Image Process.*, vol. 16, pp. 2261–2272, 2019.

[49] O. Udoudo, "Modelling the efficiency of an automated sensor-based sorter," Ph.D. dissertation, Univ. Exeter, Exeter, U.K., 2010.

[50] T. Arnold and K.-U. Vieth, "Die Auswahl von Ausblasventilen für optische Sortiersysteme," *Schttgut*, vol. 19, no. 4, pp. 54–58, 2013.

[51] E. Gülcan, "A novel approach for sensor based sorting performance determinationz," *Minerals Eng.*, vol. 146, 2020, Art. no. 106130.

Georg Maier received the M.Sc. degree in computer science from Utrecht University, Utrecht, The Netherlands, in 2013.

His research assistant with the Fraunhofer Institute of Optronics, System Technologies and Image Exploitation IOSB, Karlsruhe, Germany. His research interests include different aspects of image processing, in particular algorithmic aspects, with a focus on real-time capabilities.
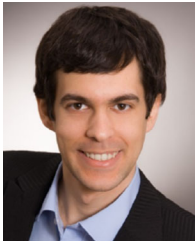
Florian Pfaff (Member, IEEE) received the Diploma and Ph.D. degrees in computer science from Karlsruhe Institute of Technology, in 2013 and 2018, respectively.

He is currently a Postdoctoral Researcher at the Intelligent Sensor-Actuator-Systems Laboratory at the Karlsruhe Institute of Technology. His current research interests include a variety of estimation problems such as filtering on nonlinear manifolds, multitarget tracking, and estimation in the presence of both stochastic and non-stochastic uncertainties.

Christoph Pieper is currently a Research Assistant with the Department of Energy Plant Technology, Ruhr University Bochum, Bochum, Germany. His current research interests include numerical simulation of fluidized particle systems with the discrete element method and computational fluid dynamics.

Robin Gruna is currently a Research Group Manager with the Fraunhofer Institute of Optronics, System Technologies and Image Exploitation IOSB, Karlsruhe, Germany. His current research interests include spectral imaging, machine learning and computational imaging.

Benjamin Noack (Member, IEEE) is currently a Senior Researcher with the Intelligent Sensor-Actuator-Systems Laboratory, Karlsruhe Institute of Technology (KIT), Karlsruhe, Germany. His research interests include multisensor data fusion, distributed and decentralized Kalman filtering, combined stochastic and set-membership approaches to state estimation, and event-based systems.

Harald Kruggel-Emden received the Diploma (MS) and Ph.D. degrees in mechanical engineering from Ruhr-Universität Bochum, Bochum, Germany, in 2003 and 2007, respectively.

He is currently a Professor and the Head with the Department of Mechanical Process Engineering and Solids Processing, Technical University of Berlin, Berlin, Germany. His currently research interests include discrete element modeling with coupled fluid flow, material preparation and drying technology, bulk solids handling, and chemical looping combustion.

Thomas Längle is currently an Adjunct Professor with the Karlsruhe Institute of Technology (KIT), Karlsruhe, Germany, and the Head of the business unit "Vision Based Inspection Systems" with the Fraunhofer IOSB, Karlsruhe. His current research interests include different aspects of image processing and real-time algorithms for inspection systems.

Uwe D. Hanebeck (Fellow, IEEE) received the Ph.D. and the habilitation degrees both in electrical engineering from the Technical University in Munich, Munich, Germany, in 1997 and 2003, respectively.

He is currently a Chaired Professor of Computer Science with the Karlsruhe Institute of Technology (KIT), Karlsruhe, Germany, and the Director of the Intelligent Sensor-Actuator-Systems Laboratory. He is an author or coauthor of more than 480 publications in various high-ranking journals and conferences and an IEEE Fellow. His current research interests include the areas of information fusion, nonlinear state estimation, stochastic modeling, system identification, and control with a strong emphasis on theory-driven approaches based on stochastic system theory and uncertainty models.

Siegmar Wirtz is currently the Deputy Head with the Department of Energy Plant Technology, Ruhr University Bochum, Bochum, Germany. His current research interests include numerical simulation of reactive gas-solid flows, extension of commercial CFD-Codes, discrete element modelling with coupled fluid flow.

Viktor Scherer is currently the Head with the Department of Energy Plant Technology, Ruhr University Bochum. His current research interests include energetic conversion of fossil fuels and biomass as well as related industrial applications and experimental and theoretical investigation of energy and high temperature processes.

Jürgen Beyerer (Member, IEEE) has been a Full Professor for informatics with the Institute for Anthropomatics and Robotics, Karlsruhe Institute of Technology (KIT), Karlsruhe, Germany, since March 2004 and the Director of the Fraunhofer Institute of Optronics, System Technologies and Image Exploitation (IOSB) in Ettlingen, Karlsruhe, Ilmenau, Lemgo. Görlitz. He is Spokesman of the Fraunhofer Group for Defense and Security VVS and he is member of Acatech, National Academy of Science and Engineering. He is the Head of Team 7 of the platform Lernende Systeme and Spokesman of the Competence Center Robotic Systems for Decontamination in Hazardous Environments. His current research interests include automated visual inspection, signal and image processing, pattern recognition, metrology, information theory, machine learning, system theory security, autonomous systems and automation.